Solar Cells

DOI: 10.1002/anie.201406190

Efficient Solar Cells Sensitized by Porphyrins with an Extended Conjugation Framework and a Carbazole Donor: From Molecular Design to Cosensitization**

*Yueqiang Wang, Bin Chen, Wenjun Wu, Xin Li, Weihong Zhu, He Tian, and Yongshu Xie**

Abstract: *Porphyrin dyes containing the carbazole electron donor have been designed and optimized by wrapping the porphyrin framework, introducing an additional ethynylene bridge to extend the wavelength range of light absorption, and further suppression of the dye aggregation by introducing additional alkoxy chains. Application of a cosensitization approach results in improved current density (J_{sc}) and open-circuit voltage (V_{oc}) values, thus achieving the highest cell efficiency of 10.45 %. This work provides an effective combined strategy of molecular design and cosensitization for developing efficient dye-sensitized solar cells (DSSCs). In addition, carbazole has been demonstrated to be a promising donor for porphyrin sensitizers.*

Dye-sensitized solar cells (DSSCs) have been widely investigated because of their low production cost, ease of fabrication, and relatively high solar energy conversion efficiencies.[1] In recent years, significant efforts have been devoted to improving cell efficiencies.[2] In this respect, many efficient sensitizers with donor–π-acceptor frameworks have been developed.[3] Among them, porphyrins have received increasing attention because of their strongly absorbing Soret bands ($\lambda = 400$–450 nm) and moderately intense Q bands ($\lambda =$ 550–650 nm) which cover the visible to the near-IR region of the electromagnetic spectrum.[4] Additionally, their chemical structures can be systematically modified to understand the effect of structural properties on cell efficiencies.[2c,5] Until recently, highly efficient porphyrin sensitizers have typically been functionalized with two bis(*ortho*-alkoxy)-wrapped *meso*-phenyl groups for reducing dye aggregation, and an ethynyl benzoic acid group as the acceptor, a strategy which was pioneered and developed by Diau and Yeh et al.[5,6] This year, the highest DSSC efficiencies of 13.0 % and 12.75 % have been reported by Grätzel and co-workers for porphyrin dyes with octyloxy-wrapped structures, utilizing a benzothiadiazole bridge between the ethynyl and benzoic acid moieties, and using a cobalt-based electrolyte.[7]

In the design of efficient dyes, one of the most commonly encountered problems is the relatively weak absorption of light in the near-IR region.[8] To overcome this problem, an additional ethynylene bridge may be introduced to expand the π-conjugated framework and enhance the absorption. However, one adverse effect of this approach is to induce severe dye aggregation, which may lower the cell efficiency. Accordingly, in most cases, the sensitizers incorporating an additional ethynylene bridge show decreased cell efficiencies.[9,10] These observations have been a serious obstacle for designing efficient sensitizers, which was also encountered in our previous work. For example, porphyrin derivative **Q1** has an additional ethynylene bridge compared to **Q2** (Scheme 1). Thus the onset wavelength of its absorption was extended from $\lambda = 655$ nm to 695 nm, but the cell efficiency was decreased from 5.51 % to 2.22 %.[11] For porphyrin sensitizers containing a carbazole donor,[11,12] the highest efficiency is 5.74 %,[12f] which is slightly higher than that for **Q2**, but much lower than the value of 12.5 % reported for the non-porphyrin carbazole-containing dye ADEKA-1.[13] This large difference prompted us to develop efficient porphyrin sensitizers with a carbazole donor through molecular design with focus on extending the π-conjugated framework in combination with multiple anti-aggregation approaches. In addition, as porphyrins usually absorb weakly around $\lambda = 500$ nm, we further utilize a cosensitization approach[14] to enhance the efficiencies by improving the absorption in this wavelength region.

Based on these considerations and the molecular structure of **Q2**, four long alkoxy chains were introduced at the *ortho* positions of the *meso*-phenyl substituents to wrap the porphyrin framework[6] and suppress dye aggregation. Porphyrin sensitizer **XW1** (Scheme 1) demonstrated a cell efficiency of 7.13 %, significantly higher than that of **Q2**. An ethynylene bridge was then inserted between the carbazole donor and the porphyrin framework, forming molecule **XW2**, to extend the absorption wavelength range, but the cell efficiency decreased to 6.84 %. To suppress the adverse dye aggregation associated with the ethynylene bridge, methoxy or hexyloxy groups were introduced onto the phenylene group adjacent to the donor. Cell efficiencies improved, with values of 7.32 % and 7.94 % achieved for **XW3** and **XW4**, respectively. Cosensitizer **C1** (see Figure 1, inset, for molecular structure) was next employed, whose absorption peak lies at approximately $\lambda = 500$ nm. Thus, the cosensitization of **XW4** and **C1** affords the highest efficiency of 10.45 %. These results provide a molecular design strategy involving an extension of the π-conjugated framework together with

[*] Y. Q. Wang, B. Chen, Dr. W. J. Wu, Dr. X. Li, Prof. Dr. W. H. Zhu, Prof. Dr. H. Tian, Prof. Dr. Y. S. Xie
Key Laboratory for Advanced Materials and Institute of Fine Chemicals
East China University of Science and Technology
Shanghai 200237 (P. R. China)
E-mail: yshxie@ecust.edu.cn

[**] This work was supported by NSFC/China (21072060, 91227201), National Basic Research 973 Program (2013CB733700), the Oriental Scholarship (NCET-11-0638), and the Fundamental Research Funds for the Central Universities (WK1013002).

Supporting information for this article is available on the WWW under http://dx.doi.org/10.1002/anie.201406190.

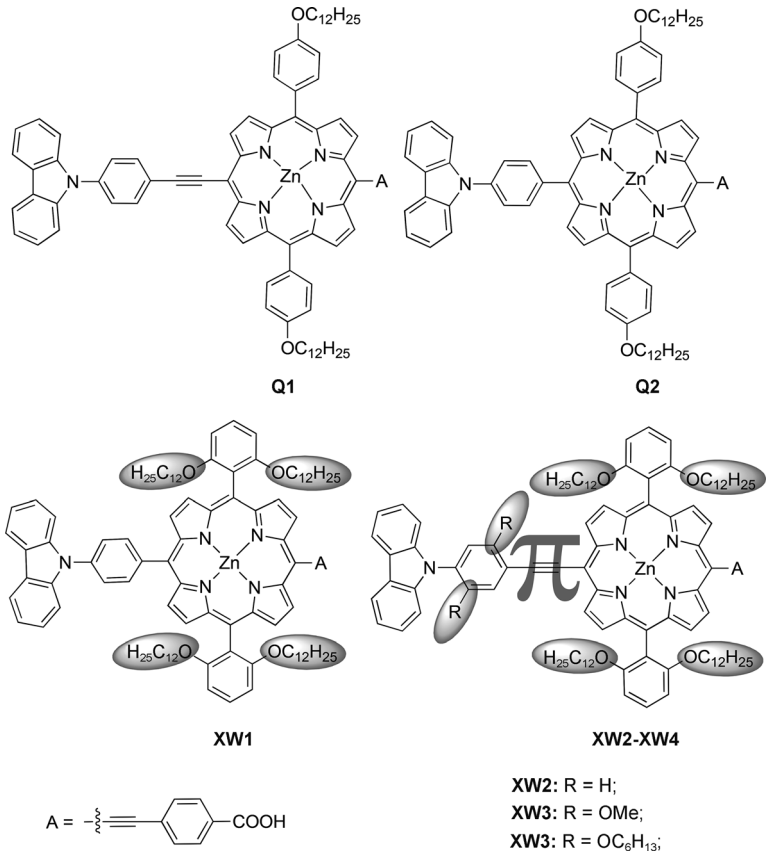

Scheme 1. Molecular structures of **XW1**–**XW4** and previously reported molecules **Q1** and **Q2**.

multiple suppression of dye aggregation. The combination of the optimized dye with a cosensitization approach is effective for developing efficient DSSCs.

The carbazole donor moiety was attached at the *meso*-position of the porphyrin unit by Suzuki or Sonogashira cross-coupling reactions (see the Supporting Information for synthetic details). The acceptor moiety was then introduced by a Sonogashira cross-coupling reaction as the corresponding acid ester. Finally, the target sensitizers were obtained through hydrolysis of the esters. The compounds were characterized using ^{1}H NMR and ^{13}C NMR spectroscopy and HRMS (Figures S1–S42 in the Supporting Information).

The UV/Vis absorption spectra of the dyes in THF are shown in Figure 1 and the corresponding data are listed in Table S1 (Supporting Information). The absorption spectra of the porphyrin dyes have features which are typical of porphyrins, with an intense Soret band in the range of $\lambda =$ 400–500 nm and less intense Q bands in the range $\lambda = 550$–700 nm. The high molar absorption coefficients fulfil the requirement for a DSSC sensitizer. Compared with **XW1**, the additional ethynylene bridges in derivatives **XW2**–**XW4** were observed to induce an obvious red shift of both the Soret and the Q bands. The additional alkoxy groups in **XW3** and **XW4** induced a slight red shift of approximately 4 nm relative to **XW2**. All of the porphyrin dyes demonstrate very weak absorption between $\lambda = 480$ and 550 nm. In contrast, cosensitizer **C1** demonstrates a broad absorption peak at approximately $\lambda = 500$ nm, which compensates well the poor absorption of the porphyrin dyes in this region and indicates that **C1** may be a good cosensitizer for the porphyrin dyes. When **XW1**–**XW4** were adsorbed onto the TiO_2 films, the spectra were significantly broadened (see Figure S43), which is favorable for light harvesting.

Cyclic voltammetry (Figure S44) was measured to evaluate the possibility of electron transfer from the excited dye molecules to the conduction band of TiO_2, and the corresponding data are summarized in Table S2. For porphyrins **XW1**–**XW4**, similar HOMO levels of 0.87, 0.85, 0.82, and 0.83 V, respectively, were calculated. The LUMO levels of **XW1**–**XW4** were estimated to be −1.09, −1.02, −1.04, and −1.03 V, respectively. The fact that the HOMO levels are comparable can be attributed to the similar electron-donating ability of the donors in the four dyes. Compared with **XW1**, the additional ethynylene bridges in **XW2**–**XW4** caused a decrease in the HOMO–LUMO energy gaps, resulting in a red shift of the absorption bands, and relatively positive LUMO levels. The LUMO levels of all these dyes lie above the conduction band of TiO_2 (−0.5 V versus NHE), and the HOMO levels lie well below the iodide/triiodide redox potential value (0.4 V versus NHE; see Figure S45). These results indicate that the electron injection and dye regeneration processes are thermodynamically feasible for each of these dyes.[15]

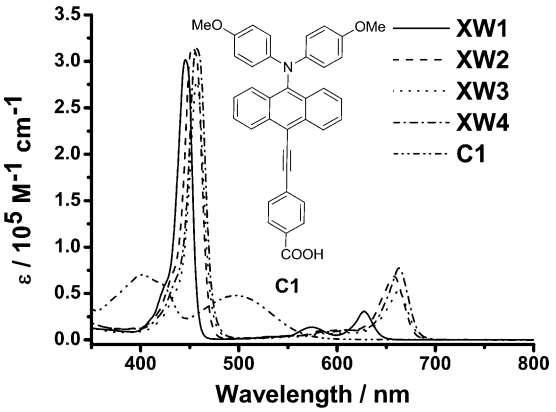

Figure 1. UV/Vis and near-IR absorption spectra of dyes **XW1**–**XW4** and cosensitizer **C1** in THF. Inset: molecular structure of **C1**.

Density functional theory (DFT) calculations were employed to understand the electron-density distributions of the frontier orbitals of the dyes. The corresponding molecular orbital profiles are shown in Figure S46. As expected, the electron densities of the HOMO orbitals of the porphyrin dyes are mainly delocalized between the donor and the porphyrin framework, whereas the LUMO orbitals are predominantly delocalized over the anchoring group and

the porphyrin framework. Thus, the electron transfer from the HOMO to the LUMO can easily result in electron redistribution from the donor to the anchoring moiety. Therefore, the electron injection from the LUMO to the conduction band of TiO_2 is theoretically feasible. Consequently, we fabricated DSSCs using these dyes as the sensitizers.

The current-density–voltage (J–V) curves (Figure 2a) of the DSSCs based on the individual porphyrin dyes were measured under simulated AM1.5 G irradiation (100 mW cm^{-2}), and the photovoltaic parameters are summarized in Table 1. The solar-to-electric power conversion efficiencies (PCE) for dyes **XW1**–**XW4** lie in the range of 6.84–7.94%, which are significantly higher than the values of 2.22% and 5.51% measured for **Q1** and **Q2**, respectively. These results may be attributed to the effective suppression of dye aggregation by the dodecoxy chains at the *ortho* positions of the *meso*-phenyl substituents. As a result, **XW1** exhibits a PCE of 7.13%. Upon introduction of an additional ethynylene bridge, the PCE falls to 6.84% for **XW2**, despite the fact its onset of absorption occurs at $\lambda = 698$ nm, at much longer wavelength than for **XW1** ($\lambda = 664$ nm). The decreased efficiency measured for **XW2** may be related to the more severe dye aggregation caused by the extended π-conjugated framework.[9] To further suppress the dye aggregation and thus improve the cell efficiency, two additional methoxy and hexyloxy chains were introduced to afford derivatives **XW3** and **XW4**, respectively. The corresponding PCE values were successively improved to 7.32% and 7.94% for **XW3** and **XW4**, respectively. These values are higher than that of **XW1**, indicating that efficient sensitizers can be designed by combining an additional ethynylene bridge with extra alkoxy chains. By this approach, the adverse dye aggregation effect which accompanies the extension of the π-conjugated framework can be suppressed, and thus the cell efficiency may be improved.

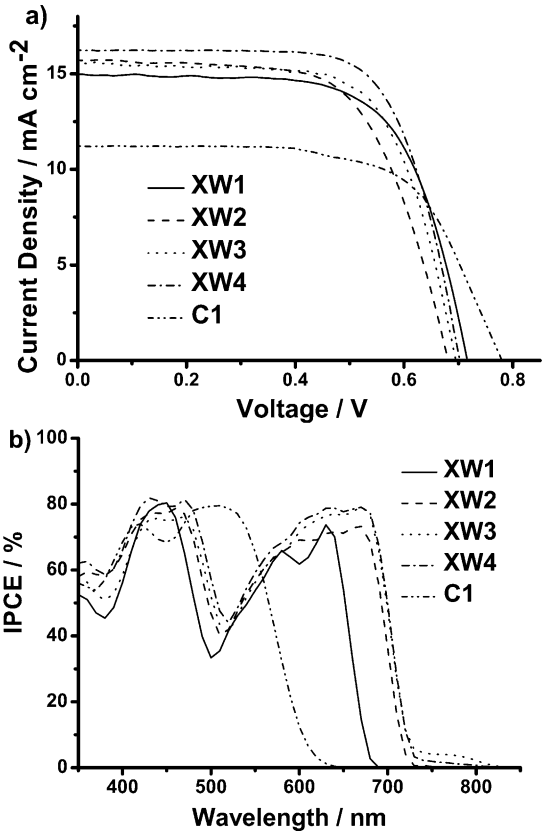

Figure 2. a) Current-density–voltage (J–V) curves and b) IPCE action spectra for the DSSCs based on **XW1**–**XW4** and **C1**.

Table 1: Photovoltaic parameters of the DSSCs under AM1.5 G illumination (power = 100 mW cm^{-2}).

Dyes	J_{sc} [mA cm^{-2}]	V_{oc} [mV]	FF	PCE [%]
Q1[11]	5.43	570	0.72	2.22
Q2[11]	11.30	680	0.71	5.51
XW1	14.99	716	0.66	7.13
XW2	15.73	680	0.64	6.84
XW3	15.60	694	0.68	7.32
XW4	16.22	702	0.70	7.94
C1	11.21	780	0.65	5.67
XW1 + **C1**[a]	17.53	746	0.71	9.24
XW2 + **C1**[a]	18.22	697	0.70	8.96
XW3 + **C1**[a]	18.42	705	0.70	9.05
XW4 + **C1**[a]	20.15	736	0.71	10.45
N719	17.65	806	0.68	9.63

[a] The cosensitization was carried out using an optimized stepwise approach: the TiO_2 electrode was immersed in a solution of the porphyrin (0.2 mM) in a mixture of toluene and ethanol (1:4 v/v) for 10 hours and then immersed in a solution of **C1** (0.3 mM) in a mixture of chloroform and ethanol (3:7 v/v) for 1.5 hours. The cosensitized films were then assembled into DSSC devices. FF = fill factor.

Based on the efficiency data, we continued to investigate the effect of the molecular structural changes on the cell current characteristics to gain more information for further improvement of cell efficiencies. Figure 2b shows the incident photon-to-current conversion efficiency (IPCE) as a function of wavelength. All the porphyrin dyes show a broad peak around $\lambda = 450$ nm and two well-separated peaks between $\lambda =$ 550 and 700 nm, corresponding to the Soret and Q bands, respectively. Compared with **XW1**, the ethynylene bridge and the alkoxy groups in **XW2**–**XW4** red shifted the onset wavelengths of photocurrent response from $\lambda = 700$ nm to $\lambda = 750$–820 nm, resulting in the current density increase from 14.99 to 15.60–16.22 mA cm^{-2} (Table 1).

The IPCE curves for **XW1**–**XW4** exhibit low values around $\lambda = 500$ nm, with the lowest value lying between 33% and 44%, which may be as a result of the weak absorption of the porphyrin dyes around $\lambda = 500$ nm. These observations may be unfavorable for improving the cell efficiencies. In contrast, **C1** shows an intense absorption band in this spectral region (Figure 2b), indicating that **C1** may be an ideal cosensitizer to compensate the absorption of the porphyrin dyes in this spectral region. Thus, more DSSCs were fabricated by employing the cosensitization approach. The photovoltaic behavior and corresponding parameters are shown in Figure 3 and Table 1. As expected, the lower IPCE values at approximately $\lambda = 500$ nm increased significantly, with the values remaining higher than 58% in this region (Figure 3b). As a result, the cosensitized devices show

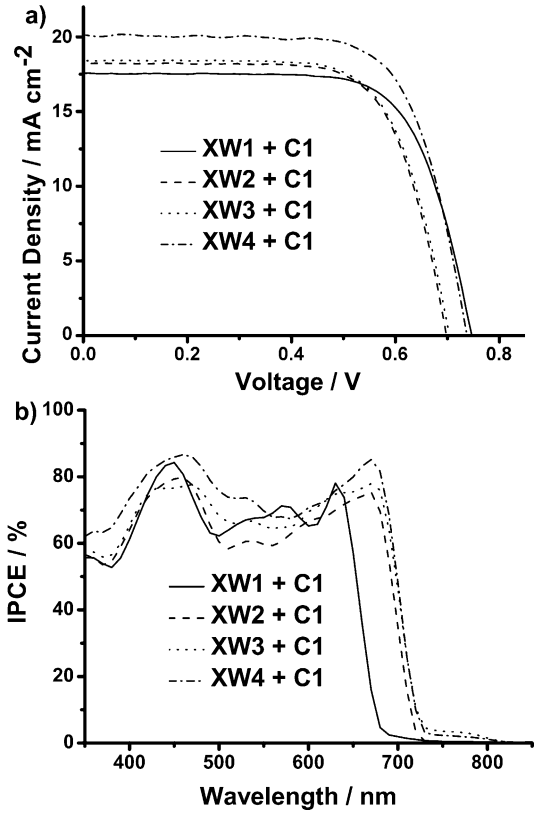

Figure 3. a) Current-density–voltage (*J*–*V*) curves and b) IPCE action spectra for the cosensitized DSSCs.

enhanced current density values (J_{sc}) compared with the corresponding individual porphyrin-sensitized devices. The onset wavelengths of photocurrent response for the cosensitized cells containing **XW2**–**XW4** vary in the range of $\lambda = 750$–820 nm, which is significant longer than that of $\lambda = 720$ nm observed for **XW1** because of the presence of the additional ethynylene bridge. In agreement with these observations, the J_{sc} values for the cosensitized cells of **XW2**–**XW4** lie in the range of 18.22–20.15 mA cm^{-2}, larger than the corresponding value for **XW1** (17.53 mA cm^{-2}).

For most cosensitization systems,[16] the open-circuit voltage (V_{oc}) is intermediate in value between those of the individual single-dye-sensitized cells. The relatively high V_{oc} value of 780 mV observed for the cells of **C1** resulted in enhanced V_{oc} values of 697–746 mV for the cosensitized DSSCs compared to those of the corresponding individual porphyrin-sensitized devices (V_{oc} values in the range 680–716 mV). In addition, high PCE values of 8.96–10.45 % were achieved for the cosensitization of **XW1**–**XW4** with **C1**. It is clear that this cosensitization approach results in enhanced J_{sc}, V_{oc}, and efficiencies for cells employing the porphyrin dyes.

To investigate the effect of the TiO_2 conduction band shift and the electron transport and charge recombination processes on V_{oc}, electrochemical impedance spectroscopy (EIS) measurements were performed as a function of potential bias. By fitting the EIS spectra, the chemical capacitance (C_μ), interfacial charge-transfer resistance (R_{CT}), and the electron lifetime (τ) can be determined.[17] Figure S47a (Supporting Information) shows that the range of C_μ values lie in the order of **XW2** < **XW1** < **XW3** ≈ **XW4**, indicating a sequential positive shift of the conduction band edge.[7a,16b,17] At a given voltage bias, the fitted R_{CT} and τ values lie in the order of **XW2** < **XW3** < **XW4** < **XW1** (Figures S47b,c), showing the same order of decreasing charge recombination rate and increasing electron lifetime.[17] The cosensitized DSSCs also demonstrated the same trend (Figure S48), which is consistent with the V_{oc} values measured for the cosensitized DSSCs. As compared with the other three dyes, the most negative TiO_2 conduction band edge of **XW2** tends to increase the V_{oc} value.[7a,16b,17] On the contrary, the shortest electron lifetime tends to decrease the V_{oc} value. As a result of the contradictory effects, derivative **XW2** demonstrates the lowest V_{oc} value of 680 mV, indicating that the V_{oc} value is predominantly determined by the charge recombination process, rather than the position of the TiO_2 conduction band.

In addition to high cell efficiencies, the photostability of sensitizers is an important parameter for the practical application of DSSCs.[18] To investigate photostabilities, the dyes adsorbed on nanocrystalline TiO_2 films were illuminated with simulated solar light without redox mediators for 30 minutes (Figure S49). The absorption of all the dyes was found to be only slightly decreased relative to the initial value, indicating that all four porphyrin dyes have satisfactory photostability.

Our results clearly show that the wrapping at the *ortho* positions of the *meso*-substituents is effective for improving the V_{oc} and J_{sc} values, as well as the cell efficiencies. Thus, the cells based on **XW1**–**XW4** showed significantly improved efficiencies (6.84–7.94 %) compared with those of **Q1** and **Q2** (2.22 % and 5.51 %). Compared with **XW1**, the ethynylene bridge in **XW2** is favorable to induce an extension of the absorption spectral range to a longer wavelength. Consequently, the J_{sc} values are improved from 14.99 to 15.73 mA cm^{-2}, but the V_{oc} values decrease from 716 to 680 mV. This effect is a result of the enhanced charge recombination associated with the more severe dye aggregation in **XW2** caused by its larger conjugated framework, thus resulting in a decrease of the cell efficiency from 7.13 % to 6.84 %. The methoxy and hexyloxy groups in **XW3** and **XW4** are favorable for suppressing the adverse dye-aggregation effect, giving rise to improved V_{oc} values of 694 and 702 mV, respectively. Compound **XW4** demonstrated the highest cell efficiency, with a value of 7.94 %. Further application of the cosensitizer **C1** with **XW1**–**XW4** significantly improved the J_{sc} values to 17.53–20.15 mA cm^{-2} and slightly improved the V_{oc} values to 705–746 mV. Finally, the cell efficiencies were improved to 8.96–10.45 %, showing the best performance for carbazole-based porphyrin-sensitized solar cells.

In summary, efficient porphyrin sensitizers have been developed by using a carbazole electron donor, and molecular design strategies have been systematically employed to optimize the dye structures by wrapping the porphyrin framework with four long alkoxy chains, introducing an ethynylene bridge, and further suppression of dye aggregation by employing additional alkoxy chains. Finally, a non-porphyrin dye **C1**, with a high V_{oc} value and strong absorption at approximately $\lambda = 500$ nm, was used as the cosensitizer. This

cosensitization approach significantly enhanced the J_{sc} value and slightly enhanced the V_{oc}. Thus, the highest cell efficiency of 10.45% was achieved. This value is higher than that obtained for the ruthenium dye N719[19] (Table 1), and significantly higher than the best efficiency of 5.74% previously reported for porphyrin dyes containing a carbazole donor.[12f] In conclusion, this work provides an effective combined strategy of molecular design and cosensitization for developing efficient DSSCs. We have also demonstrated for the first time that carbazole is a promising donor moiety for developing efficient porphyrin sensitizers. Considering the structural characteristics and the energy-level distribution, it is anticipated that cell efficiencies may be further improved by using a benzothiadiazole-bridged acceptor group as well as the Co^{3+}/Co^{2+} redox electrolyte,[7] which is under investigation in our group.

Received: June 13, 2014
Revised: July 3, 2014
Published online: August 11, 2014

Keywords: dyes/pigments · energy conversion · porphyrins · sensitizers · solar cells

[1] B. O'Regan, M. Grätzel, *Nature* **1991**, *353*, 737 – 740.
[2] a) C. C. Chou, F. C. Hu, H. H. Yeh, H. P. Wu, Y. Chi, J. N. Clifford, E. Palomares, S. H. Liu, P. T. Chou, G. H. Lee, *Angew. Chem.* **2014**, *126*, 182 – 187; *Angew. Chem. Int. Ed.* **2014**, *53*, 178 – 183; b) Y. Z. Wu, W. H. Zhu, *Chem. Soc. Rev.* **2013**, *42*, 2039 – 2058; c) L. L. Li, E. W. G. Diau, *Chem. Soc. Rev.* **2013**, *42*, 291 – 304.
[3] a) M. Zhang, Y. Wang, M. Xu, W. Ma, R. Li, P. Wang, *Energy Environ. Sci.* **2013**, *6*, 2944 – 2949; b) X. Ren, S. Jiang, M. Cha, G. Zhou, Z. S. Wang, *Chem. Mater.* **2012**, *24*, 3493 – 3499; c) J. Liu, Y. Numata, C. Qin, A. Islam, X. Yang, L. Y. Han, *Chem. Commun.* **2013**, *49*, 7587 – 7589.
[4] C. L. Wang, Y. C. Chang, C. M. Lan, C. F. Lo, E. W. G. Diau, C. Y. Lin, *Energy Environ. Sci.* **2011**, *4*, 1788 – 1795.
[5] T. Bessho, S. M. Zakeeruddin, C. Y. Yeh, E. W. G. Diau, M. Grätzel, *Angew. Chem.* **2010**, *122*, 6796 – 6799; *Angew. Chem. Int. Ed.* **2010**, *49*, 6646 – 6649.
[6] a) T. Ripolles-Sanchis, B. Guo, H. Wu, T. Pan, H. Lee, S. Raga, F. Santiago, J. Bisquert, C. Y. Yeh, E. W. G. Diau, *Chem. Commun.* **2012**, *48*, 4368 – 4370; b) C. Wang, C. Lan, S. Hong, Y. Wang, T. Pan, C. Chang, H. Kuo, M. Kuo, E. W. G. Diau, C. Y. Lin, *Energy Environ. Sci.* **2012**, *5*, 6933 – 6940.
[7] a) S. Mathew, A. Yella, P. Gao, R. H. Baker, B. F. E. Curchod, N. A. Astani, I. Tavernelli, U. Rothlisberger, M. K. Nazeeruddin, M. Grätzel, *Nat. Chem.* **2014**, *6*, 242 – 247; b) A. Yella, C. L. Mai, S. M. Zakeeruddin, S. N. Chang, C. H. Hsieh, C. Y. Yeh, M. Grätzel, *Angew. Chem.* **2014**, *126*, 3017 – 3021; *Angew. Chem. Int. Ed.* **2014**, *53*, 2973 – 2977.
[8] a) K. Lim, M. J. Ju, J. Song, I. T. Choi, K. Do, H. Choi, K. Song, H. K. Kim, J. Ko, *ChemSusChem* **2013**, *6*, 1425 – 1431; b) W. H. Zhu, Y. Z. Wu, S. Wang, W. Q. Li, X. Li, J. Chen, Z. S. Wang, H. Tian, *Adv. Funct. Mater.* **2011**, *21*, 756 – 763.
[9] a) C. W. Lee, H. P. Lu, C. M. Lan, Y. L. Huang, Y. R. Liang, W. N. Yen, Y. C. Liu, Y. S. Lin, E. W. G. Diau, C. Y. Yeh, *Chem. Eur. J.* **2009**, *15*, 1403 – 1412; b) C. P. Hsieh, H. P. Lu, C. L. Chiu, C. W. Lee, S. H. Chuang, C. L. Mai, W. N. Yen, S. J. Hsu, E. W. G. Diau, C. Y. Yeh, *J. Mater. Chem.* **2010**, *20*, 1127 – 1134; c) S. L. Wu, H. P. Lu, H. T. Yu, S. H. Chuang, C. L. Chiu, C. W. Lee, E. W. G. Diau, C. Y. Yeh, *Energy Environ. Sci.* **2010**, *3*, 949 – 955; d) J. H. Delcamp, Y. Shi, J. H. Yum, T. Sajoto, E. Dell'Orto, S. Barlow, M. K. Nazeeruddin, S. R. Marder, M. Grätzel, *Chem. Eur. J.* **2013**, *19*, 1819 – 1827.
[10] For some exceptions, see: a) J. He, W. J. Wu, J. L. Hua, Y. Jiang, S. Qu, J. Li, Y. Long, H. Tian, *J. Mater. Chem.* **2011**, *21*, 6054 – 6062; b) J. Luo, M. Xu, R. Li, K. W. Huang, C. Jiang, Q. Qi, W. Zeng, J. Zhang, C. Chi, P. Wang, J. Wu, *J. Am. Chem. Soc.* **2014**, *136*, 265 – 272.
[11] Y. Q. Wang, X. Li, B. Liu, W. J. Wu, W. H. Zhu, Y. S. Xie, *RSC Adv.* **2013**, *3*, 14780 – 14790.
[12] a) Y. Liu, H. Lin, J. Li, J. T. Dy, K. Tamaki, J. Nakazaki, D. Nakayama, C. Nishiyama, S. Uchida, T. Kubo, H. Segawa, *Phys. Chem. Chem. Phys.* **2012**, *14*, 16703 – 16712; b) Y. Liu, H. Lin, J. T. Dy, K. Tamaki, J. Nakazaki, D. Nakayama, S. Uchida, T. Kubo, H. Segawa, *Chem. Commun.* **2011**, *47*, 4010 – 4012; c) R. B. Ambre, G. F. Chang, M. R. Zanwar, C. F. Yao, E. W. G. Diau, C. H. Hung, *Chem. Asian J.* **2013**, *8*, 2144 – 2153; d) X. Xue, W. Zhang, N. Zhang, C. Ju, X. Peng, Y. Yang, Y. Liang, Y. Feng, B. Zhang, *RSC Adv.* **2014**, *4*, 8894 – 8900; e) L. Favereau, J. Warnan, F. B. Anne, Y. Pellegrin, E. Blart, D. Jacquemin, F. Odobel, *J. Mater. Chem. A* **2013**, *1*, 7572 – 7575; f) Y. Liu, H. Lin, J. T. Dy, K. Tamaki, J. Nakazaki, C. Nishiyama, S. Uchida, H. Segawa, J. Li, *J. Phys. Chem. C* **2014**, *118*, 1426—1435.
[13] K. Kakiage, Y. Aoyama, T. Yano, T. Otsuka, T. Kyomen, M. Unno, M. Hanaya, *Chem. Commun.* **2014**, *50*, 6379 – 6381.
[14] C. L. Wang, J. Y. Hu, C. H. Wu, H. H. Kuo, Y. C. Chang, Z. J. Lan, H. P. Wu, E. W. G. Diau, C. Y. Lin, *Energy Environ. Sci.* **2014**, *7*, 1392 – 1396.
[15] D. P. Hagberg, J. H. Yum, H. Lee, F. D. Angelis, T. Marinado, K. M. Karlsson, R. H. Baker, L. C. Sun, A. Hagfeldt, M. Grätzel, M. K. Nazeeruddin, *J. Am. Chem. Soc.* **2008**, *130*, 6259 – 6266.
[16] a) J. J. Cid, J. H. Yum, S. R. Jang, M. K. Nazeeruddin, E. M. Ferrero, E. Palomares, J. J. Ko, M. Grätzel, T. Torres, *Angew. Chem.* **2007**, *119*, 8510 – 8514; *Angew. Chem. Int. Ed.* **2007**, *46*, 8358 – 8362; b) A. Yella, H. W. Lee, H. N. Tsao, C. Y. Yi, A. K. Chandiran, M. K. Nazeeruddin, E. W. G. Diau, C. Y. Yeh, S. M. Zakeeruddin, M. Grätzel, *Science* **2011**, *334*, 629 – 634.
[17] Y. Shi, M. Liang, L. Wang, H. Han, L. You, Z. Sun, S. Xue, *ACS Appl. Mater. Interfaces* **2013**, *5*, 144 – 153.
[18] R. Katoh, A. Furube, S. Mori, M. Miyashita, K. Sunahara, N. Koumura, K. Hara, *Energy Environ. Sci.* **2009**, *2*, 542 – 546.
[19] M. K. Nazeeruddin, S. M. Zakeeruddin, R. H. Baker, M. Jirousek, P. Liska, N. Vlachopoulos, V. Shklover, C. H. Fischer, M. Grätzel, *Inorg. Chem.* **1999**, *38*, 6298—6305.

